SAHARAN DESERT DUST MICROPHYSICAL PROPERTIES FROM PRINCIPLE COMPONENT ANALYSIS (PCA) INVERSION OF RAMAN LIDAR DATA OVER WESTERN EUROPE

M. de Graaf and D. P. Donovan[1] and A. Apituley[2]

[1]*Royal Netherlands Meteorological Institute (KNMI). Wilhelminalaan 10, 3732 GK De Bilt, The Netherlands, E-mail: graafdem@knmi.nl. donovan@knmi.nl*

[2]*National Institute for Public Health and the Environment (RIVM), Antonie van Leeuwenhoeklaan 9, 3721 MA Bilthoven, The Netherlands E-mail:apituley@rivm.nl*

ABSTRACT

A large Saharan desert dust outbreak in May 2009 was detected using a Raman lidar, deployed in Leipzig, Germany. The optical data showed three distinct vertical layers, two with little spectral variation in the extinction, and one with a large spectral variation in both the scattering ratio and extinction measurements. Furthermore, the layer with the large spectral variation showed much larger particle depolarisation ratios and lidar ratios than the two other layers, which is typical for Saharan desert dust. Backtrajectory and dust distribution forecast and hindcast models showed that the different layers all originated over the Sahara, but had different transport histories. The measurements were inverted to derive microphysical properties of the particles in the layers. The method derives integral properties of the aerosols using principle component analysis, adapted for use in the troposphere. It accounts for varying refractive indices of the ambient aerosols, as shown in this paper.

1. SAHARAN DUST OUTBREAK

In May 2009 a large outbreak of Saharan desert dust was advected over Europe and detected using a Raman lidar. Figure 1 shows the dust optical depth at 550 nm and the 3000 m wind analysis on 23 May 2009, 12 UTC, over northern Africa and western Europe, and the 6 h forecast for 25 May 2009, 18 UTC, from the BSC/DREAM model [Nickovic et al., 2001]. It shows the origin of a dust plume over Algeria on the 23rd, which caused relatively high aerosol optical thicknesses (AOT) over western Europe in subsequent days. On 25 May 2009 layers of Saharan dust were observed over Leipzig, Germany, (51.35°N, 12.43°E, indicated by a black star in Fig. 1), by the Raman lidar 'Caeli'. According to Fig. 1 the Aerosol Optical Thickness (AOT) over Leipzig on 25 May 2009 around 18 UTC is about 0.75.

Backtrajectories were computed using NOAA's Hybrid Single Particle Lagrangian Integrated Trajectory (Hysplit) model [Draxler, 2003] to three days before 25 May 2009. The results are shown in Fig. 2. The dust plume is indeed advected from Morocco and Algeria to Leipzig. However, the top air parcel, ending at around 4 km altitude clearly has a different origin and history than the two air parcels arriving at 1.5 and 3 km altitude.

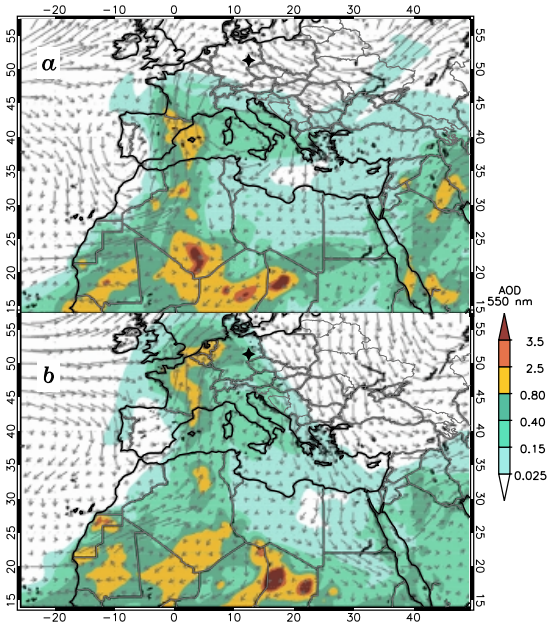

Figure 1: a) Dust optical depth at 550 nm and 3000 m wind analysis at 23 May 2009 12 UTC, and b) dust optical depth at 550 nm and 3000 m wind 6 h forecast for 25 May 2009 18 UTC, from the BSC/DREAM model.

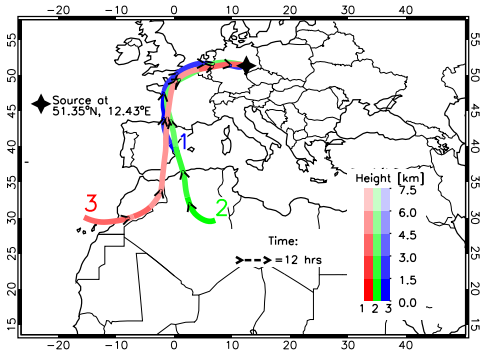

Figure 2: Three day backtrajectories ending at 25 May 2009 19 UTC at Leipzig (51.35°N, 12.43°E, indicated by the black star) from NOAA's HYSPLIT model. Package 1 (blue) ended at 1500 m asl, package 2 (green) ended at 3000 m asl and package 3 (red) ended at 4000 m asl.

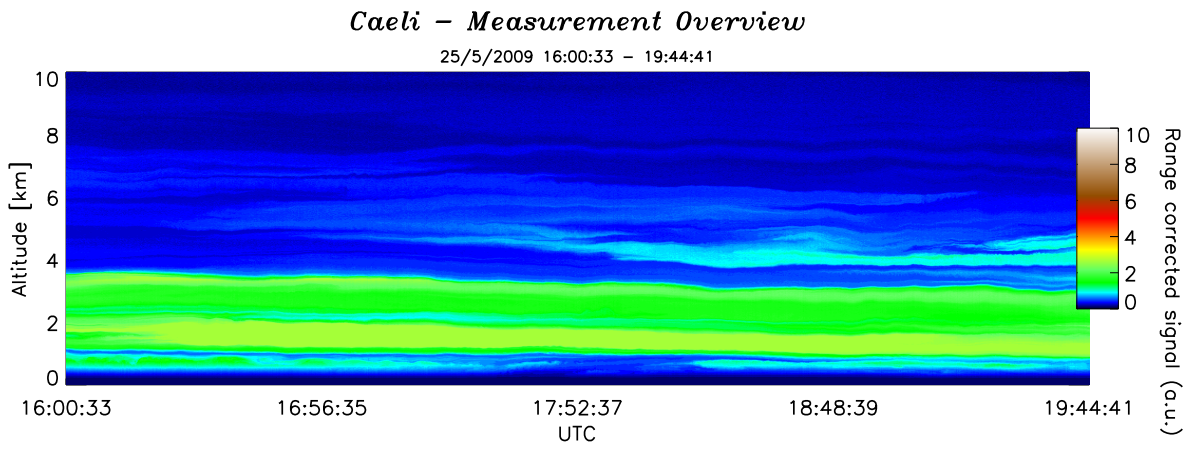

Figure 3: Caeli range-corrected returned signal at 1064 nm (arbitrary units) from 0 to 10 km on 25 May 2009, from 16:00 to 19:45 UTC.

2. RAMAN MEASUREMENTS

Caeli (CESAR Water Vapour, Aerosol and Cloud Lidar) [1] is a Raman lidar built by the National Institute for Public Health and the Environment (RIVM) and normally deployed at the Cabauw Experimental Site for Atmospheric Research (CESAR) in the Netherlands [Apituley et al., 2009]. In May 2009 it was deployed in Leipzig for an intercomparisons campaign in the framework of the European Aerosol Research LIdar NETwork (EARLINET), in which Caeli participates. Caeli uses an Nd:YAG laser to transmit light at 355, 532 and 1064 nm. The primary measurements are profiles of aerosol extinction and backscatter, relative humidity and atmospheric polarisation properties.

Figure 3 shows a Caeli measurement overview of 25 May 2009, from 16:00 to 19:45 UTC from 0 to 10 km altitude. It shows a cloud-free atmosphere, a well developed boundary layer up to almost 4 km altitude, with a layered structure, and a developing layer above the boundary layer at around 4 km altitude.

The measurements from Caeli were averaged from 16:00 to 19:45 UTC, to retrieve the average scattering ratios at 355, 532 and 1064 nm and extinction coefficients at 355 and 532 nm (Fig. 4). The scattering ratio is defined as $R = (\beta_p + \beta_m)/\beta_m$, where β_p refers to particle backscatter and β_m to molecular backscatter. Furthermore, the profiles were smoothed in the vertical using a variable sliding window. The error bars show the resolution of the sliding window in the sense that the error bars are given for each independent vertical point. The scattering ratios clearly show three distinct layers between 1 km and about 4.5 km: two layers within the boundary layer up till about 3.5 km and one layer around 4 km altitude. Note that the top layer has a different ratio of both the 355 and 532 nm scattering ratio and the 355 and 532 nm extinction, compared to those in the two lower layers. This is an indication of different refractive behaviour of the scatterer, i.e. the refractive index of the scatterers in the top layer is different from that of the lower layers, presumably caused by different types of particles.

This is shown in a different way in Figure 5, which shows the profiles of the volume depolarisation ratio, the particle depolarisation ratio and lidar ratio. The volume or

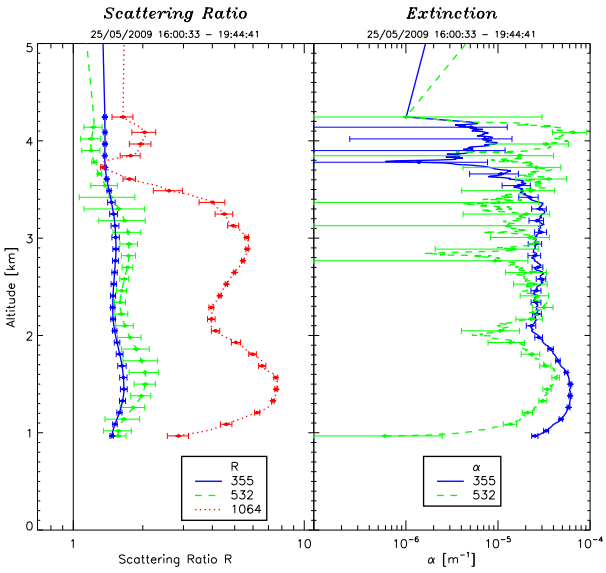

Figure 4: Scattering ratios at 355, 532 and 1064 nm and extinction at 355 and 532 nm from Caeli at Leipzig (51.35°N, 12.43°E), on 25 May 2009, averaged from 16:00 to 19:45 UTC.

[1] Latin: cælum (1) -i n. [the heavens , sky, air, climate]. Esp. [heaven] as the home of the gods; fig., [heaven] as the height of joy, renown, etc., cælum (2) -i n. [the burin or engraving tool]

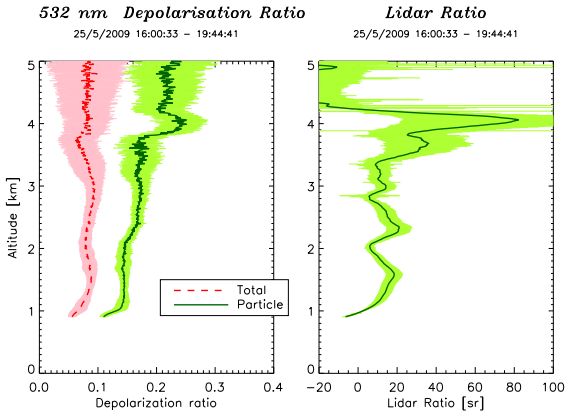

Figure 5: Total and particle depolarisation ratios and lidar ratio at 532 nm from the Caeli measurements shown in Fig. 4

total depolarisation ratio (δt) is defined as the ratio of the perpendicular ($\beta_\perp$) and the parallel ($\beta_\parallel$) part of the polarisation of the reflected light ($\delta t = \beta_\parallel/\beta_\perp$). $\beta_\perp$ and $\beta_\parallel$, measured by Caeli at 532 nm, consist of both the molecular and the particle backscatter. The molecular depolarisation ratio ($\delta m = \beta_{m_\parallel}/\beta_{m_\perp}$) can be separated from the particle depolarisation ratio ($\delta p = \beta_{p_\parallel}/\beta_{p_\perp}$) using the scattering ratio R defined above. The particle depolarisation can then be written as [e.g. Kobayashi et al., 1987]:

$$\delta p = \frac{[(R-1)\delta m + R]\,\delta t - \delta m}{\delta m R - \delta t + R - 1}. \qquad (1)$$

The lidar ratio shown in Fig. 5 is the extinction-to-backscatter ratio at 532 nm.

The particle depolarisation ratio from 1 to 3 km altitude is about 0.15-0.18, which is rather large and typical for depolarising particles. However, the layer at 4 km altitude has an even larger particle depolarisation ratio of up to about 0.25. These large depolarisation ratios are typical for transported Saharan desert dust Müller et al. [2007]. The lower layers show lidar ratio at 532 nm of about 20-22, which are values typically observed for marine aerosols in the boundary layer. The layer around 4 km altitude shows lidar ratios of up to 80 sr, which is very large. This is again indicative of desert dust, although 80 sr is larger than typical values of around 60 sr.

3. INVERSION

The measurements were inverted to retrieve integral microphysical aerosol properties to test a fast and robust principle component analysis (PCA) method [Thomason and Osborn, 1992; Donovan and Carswell, 1997], adapted for use in troposphere. Due to the limited number of extinction and backscatter measurements it is generally not feasible to retrieve the entire aerosol size distribution. The problem is mathematically under-determined and ill-posed, and inferred size distribution can have large errors. Integral properties of the aerosol size distribution on the other hand, like aerosol total volume and surface area density, are much less dependent on the employed retrieval method and measurement errors [Donovan and Carswell, 1997]. However, the refractive index of the particles must still be assumed, which makes it impracticable for use in the troposphere. Therefore, the method was extended to account for varying refractive indices.

For spherical scatterers at a given altitude and wavelength we have

$$\alpha(\lambda) = \int_0^\infty \pi r^2 Q_{\alpha,\lambda}(r) \frac{dn(r)}{dr} dr, \qquad (2)$$

and

$$\beta_\pi(\lambda) = \int_0^\infty \pi r^2 Q_{\beta_\pi,\lambda}(r) \frac{dn(r)}{dr} dr. \qquad (3)$$

where r is the particle radius, $Q_{\beta_\pi,\lambda}(r)$ is the backscatter efficiency, $Q_{\alpha,\lambda}(r)$ is the extinction efficiency, and $dn(r)/dr$ is the aerosol size distribution. Equations (2) and (3) can be rewritten as:

$$g_i = \int_0^\infty K_i(\lambda, r, m) \frac{dV(r)}{dr} dr, \qquad (4)$$

where $dV(r)/dr$ is the aerosol volume size distribution, g_i is either the backscatter or extinction measurement and K_i is the appropriate extinction or backscatter volume kernel for wavelength λ_i. Equation 4 can also be expressed in terms of extinction or backscatter surface kernels and the aerosol surface size distribution $dS(r)/dr$.

The kernel functions K_i are dependent on the refractive index of the used aerosol model. Using a set of kernel functions of different aerosol refractive indices, that are distinct and complete enough to contain the refractive index of ambient aerosols, one can use the PCA method to retrieve integral aerosol microphysical properties for tropospheric aerosols. To select the optimum kernel function from the set, a selection criterion was defined that uses the ability of the PCA method to reconstruct the extinction and backscatter measurements at the various wavelengths from a combination of the retrieved extinction and backscatter coefficients at other wavelengths. The kernel set that reconstructs the coefficients the best, also indicates the refractive index of the ambient aerosols. However, to retrieve accurate refractive indices in this way, a large set of volume kernels are needed and the results are very sensitive to measurements errors.

On the other hand, aerosol total volume and surface area density retrievals are much less sensitive to the differences in refractive indices of the ambient aerosols and those used in the kernel sets, if the kernel sets are distinct enough. We used four sets, two representing scattering

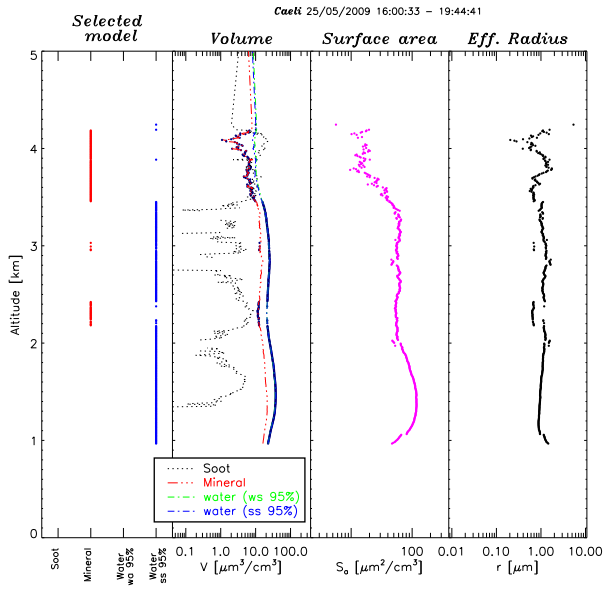

Figure 6: PCA results from the Caeli signals in Fig. 4. The left panel shows the selected model at every height. The second panel shows the total volume retrievals. The thick solid line is the selected total volume profile using the optimum kernel set at every height shown in the left panel, while the thin line show the individual profiles for the different kernel sets. The third panel shows the selected retrieved surface area profile, which was retrieved using surface kernels. The right panel shows the effective radius retrieval, derived from the retrieved volume and surface profiles shown in the second and third panels.

marine aerosols, one representing UV-absorbing desert dust aerosols, and one representing soot, absorbing at all wavelengths. Increasing the number of kernels sets does not significantly improve the results of the retrieved volume and surface parameters.

The PCA method was applied to the data shown in Figs. 4, the result is shown in Fig. 6. The left most panel shows the selected optimal kernel profile. The two layers between 1 and 2 km and 2 and about 3.5 km are retrieved as water-like aerosols, with some parts classified as mineral aerosols. Note that the total volume retrieval for water-like particles and mineral dust particles is almost equal, as shown in the next panel. The layer from about 3.5 to 4.5 km is classified as mineral aerosol for the most part. Here, the results from all kernel sets are close in terms of retrieved total volume.

4. DISCUSSION

The results in terms of refractive index for the lowest layers are very similar, while the top layer shows clearly different results, which is consistent with Figs. 4 and 5. The PCA inversion implicitly uses the differences in the 355 and 532 nm extinction ratio and the ratio of the 355 and 532 nm scattering ratio to indicate particle type quantitatively. However, even if the refractive index results are not so good, the integral size distribution results can still be good, since the kernels span a large range of refractive index.

The results from the PCA inversion show little variation in the effective particle radius for the aerosol in all layers. The backtrajectories (Fig.2) show that the air from the top layer has a distinct different history than that from the two layers beneath. This suggests that the aerosol layers found in the measurements are desert dust aerosols advected from northern Africa, with the mineral aerosols in the lowest layers possibly moistened in the boundary layer, increasing their sphericity and changing the refractive index, while the aerosols in the top layer, outside the boundary layer, retain their typical 'desert dust' signature. However, this should be confirmed by independent observations.

ACKNOWLEDGMENTS

This work was financed by the Netherlands Institute for Space Research, project number GO-2005/075.

REFERENCES

Apituley, A., K. M. Wilson, C. Potma, H. Volten and M. de Graaf (2009). Performance Assessment and Application of Caeli - A high-performance Raman lidar for diurnal profiling of Water Vapour, Aerosols and Clouds. In *Proceedings of the 8th International Symposium on Tropospheric Profiling, ISTP 8, Delft*.

Donovan, D. P. and A. I. Carswell (1997). Principle component analysis applied to multiwavelength lidar aerosol backscatter and extinction measurements. *Appl. Opt. 36* (36), 9406–9424.

Draxler, R. R. (2003). Evaluation of an ensemble dispersion calculation. *J. Appl. Meteor. 42*, 308–317.

Kobayashi, A., S. Hayashida, Y. Iwasaka, M. Yamato and A. Ono (1987). Consideration of Depolarization Ratio Measurements by Lidar - in Relation to Chemical Composition of Aerosol Particles. *J. Meteor. Soc. Japan 65* (2), 303 – 307.

Müller, D., A. Ansmann, I. Mattis, M. Tesche, U. Wandinger, D. Althausen and G. Pisani (2007). Aerosol-type-dependent lidar ratios observed with Raman lidar. *J. Geophys. Res. 112*, DOI: 10.1029/2006JD008292.

Nickovic, S., G. Kallas, A. Papadopoulos and O. Kakaliagou (2001). A model for prediction of desert dust cycle in the atmosphere. *J. Geophys. Res. 106* (D16), 18,113–18,129.

Thomason, L. W. and M. T. Osborn (1992). Lidar conversion parameters derived from sage ii extinction measurements. *Geoph. Res. Lett. 19* (16), 1655–1658.